CONF-960155--5

UCRL-JC--123537

UCRL-JC-123537
PREPRINT

2l - nl' X-ray Transitions from Neonlike Charge States of the Row 5 Metals with $39 \leq Z \leq 46$

J. E. Rice
K. B. Fournier
J. L. Terry
M. Finkenthal
E. S. Marmar
W. H. Goldstein
U. I. Safronova

This paper was prepared for submittal to the
10th APS Topical Conference on Atomic Processes in Plasmas
January 14 - 18, San Francisco, CA

March 18, 1996

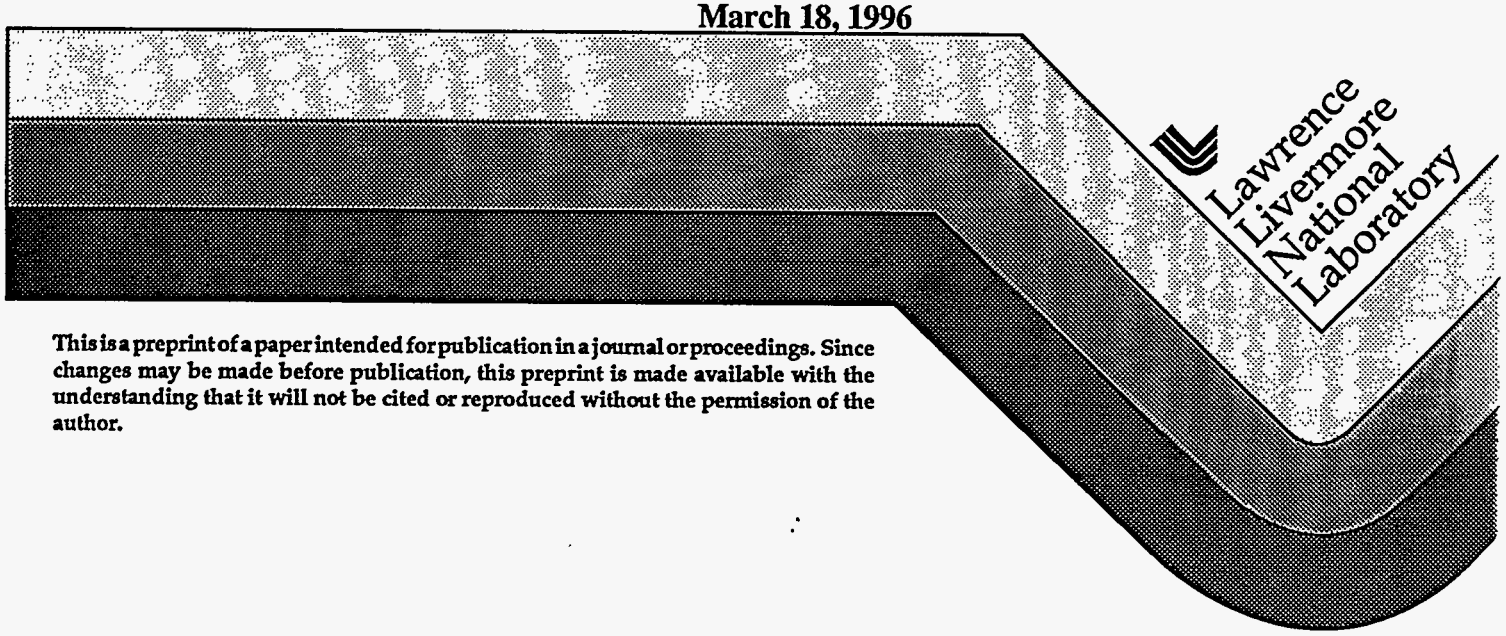

$2l$ - nl' X-ray Transitions from Neonlike Charge States of the Row 5 Metals with $39 \leq Z \leq 46$

J. E. Rice, K. B. Fournier[+], J. L. Terry, M. Finkenthal[!],
E. S. Marmar, W. H. Goldstein[+] and U.I. Safronova[*]
Plasma Fusion Center, MIT, Cambridge, MA 02139-43070

[+] *Lawrence Livermore National Laboratory, Livermore, CA 94550*
[!] *Racah Institute of Physics, The Hebrew University, Jerusalem, Israel, 91904*
[*] *Institute for Spectroscopy, Russian Academy of Sciences, Troitsk, 142092, Russia*

Abstract

X-ray spectra of $2l$ - nl' transitions with $3 \leq n \leq 12$ in the row five transition metals zirconium (Z=40), niobium (Z=41), molybdenum (Z=42) and palladium (Z=46) from charge states around neonlike have been observed from Alcator C-Mod plasmas. Accurate wavelengths (± .2 mÅ) have been determined by comparison with neighboring argon, chlorine and sulphur lines with well known wavelengths. Line identifications have been made by comparison to *ab initio* atomic structure calculations, using a fully relativistic, parametric potential code. For neonlike ions, calculated wavelengths and oscillator strengths are tabulated for 2p-nd transitions in Y (Z=39), Tc (Z=43), Ru (Z=44) and Rh (Z=45) with n = 6 and 7. The magnitude of the configuration interaction between the $(2p^5)_{\frac{1}{2}}6d_{\frac{3}{2}}$ $J = 1$ level and the $(2p^5)_{\frac{3}{2}}7d_{\frac{5}{2}}$ $J = 1$ levels is demonstrated as a function of atomic number for successive neonlike ions. Measured spectra of selected transitions in the aluminum-, magnesium-, sodium- and fluorinelike isosequences are also shown.

Introduction

Recently there has been considerable interest in x-ray transitions in high Z ions with charge states around the neonlike isosequence[1–11]. X-ray lasing[12,13] has been demonstrated in neonlike ions, and a need to understand the kinetics of this system has motivated development of very precise collisional-radiative modelling tools[14]. The identifications of many x-ray lines from neonlike ions allow high resolution experimental data to be used for benchmarking multi-electron atomic structure calculations[15–19]. Most of the work which has been

done in the past has been limited to 3-3, 2-3 and 2-4 transitions in the NeI isosequence and adjacent charge states. The high temperature, optically thin tokamak plasmas enable the measurement of many lines originating in transitions from levels having $n \geq 5$; in fact, all of the transitions in the 2p-nd series in Mo^{32+} lying under the ionization potential have been measured[10,11]. The availability of a large number of transitions in several adjacent elements provides the opportunity to study the systematics of configuration interaction effects.

In this paper are presented spectra of selected 2p-nd transitions with n between 3 and 7 in near-neonlike Zr, Nb, Mo and Pd, obtained from Alcator C-Mod plasmas[20]. A comprehensive study of numerous transitions in these elements is given in Ref. (11). The 2p-nd transitions considered here are strongly split by the j-value (in jj-coupling) of the 2p hole in the ionic core. The splitting is very apparent in the neonlike ions, where the resonance transitions with upper states containing a $2p_{\frac{1}{2}}$ hole are at much shorter wavelengths than the corresponding transitions with a $2p_{\frac{3}{2}}$ hole. This splitting can lead to significant configuration interaction when a $(2p^5)_{\frac{1}{2}}$nd orbital is close in energy to a $(2p^5)_{\frac{3}{2}}$n'd (n'>n) orbital. Interaction between the orbitals will perturb transition wavelengths and re-distribute oscillator strength within a class of transitions[21]. The magnitude of the configuration interaction between the $(2p^5)_{\frac{1}{2}}6d_{\frac{3}{2}}$ $J = 1$ level and the $(2p^5)_{\frac{3}{2}}7d_{\frac{5}{2}}$ $J = 1$ levels has been measured as a function of energy level spacing for the neonlike ions of Zr, Nb and Mo[11]. In this paper calculations are presented for these interacting levels in neonlike ions with $39 \leq Z \leq 46$.

The x-ray observations described here were obtained from the Alcator C-Mod[20] tokamak, a compact high field device with all molybdenum plasma facing components. For these measurements, the plasma parameters were in the range of $7.7 \times 10^{13}/cm^3 \leq n_{e0} \leq 2.0 \times 10^{14}/cm^3$ and $1500\ eV \leq T_{e0} \leq 3400\ eV$. A laser blow-off impurity injection system[22], which has been used to study impurity transport, was used to inject niobium, palladium and zirconium into Alcator C-Mod plasmas. The spectra presented here were recorded by a five chord, independently spatially scannable, high resolution x-ray spectrometer array[23]. Wavelength calibration[2,3] has been achieved by determining the instrumental dispersions in reference to H- and He-like argon, chlorine and sulphur lines and previously measured molybdenum[10] lines.

Ab initio atomic structure calculations for the aluminum- through fluorine-like isosequences (ground states $2p^6 3s^2 3p$ to $2s^2 2p^4$, respectively) have been performed using the RELAC code[24,25], which solves the Dirac equation by optimizing a parametric potental. RELAC has been used to calculate the full

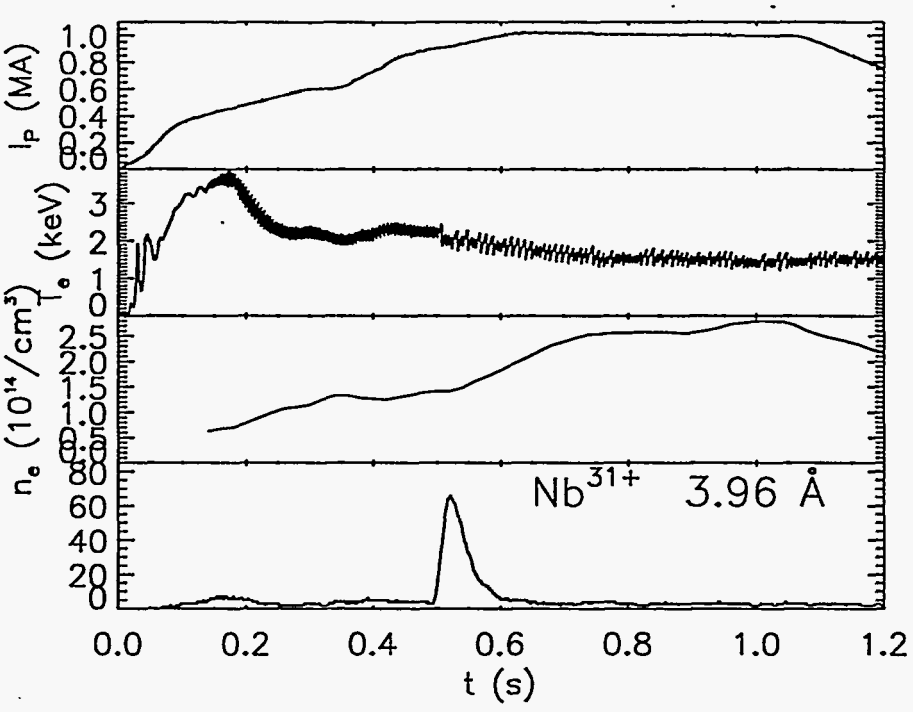

Figure 1: Plasma current, electron temperature, electron density and Nb x-ray (3.96 Å) brightness time histories in a discharge with a niobium injection at .5 sec.

multi-configuration transition wavelengths and oscillator strengths for all lines observed in this paper.

X-ray Transitions

Shown in Fig.1 are the time histories of several quantities of interest for a typical Alcator C-Mod 5.3 T, deuterium discharge. There was a niobium injection into this particular discharge at 0.5 seconds, when the plasma current was 0.9 MA, the central electron temperature was 2200 eV and the central electron density was 1.3 x 10^{14}/cm^3. The niobium stayed in the plasma for about 100 ms, as shown by the bottom frame of the figure, indicative of anomalously fast impurity transport[22]. In Fig.2 is shown an x-ray spectrum taken during an injection which demonstrates the strongest niobium line which falls within the wavelength range of the spectrometer, the $2p^6$ - $(2p^5)_{\frac{3}{2}}4d_{\frac{5}{2}}$ transition in neonlike Nb^{31+} at 3957.3 mÅ. Also apparent in this spectrum are some sodiumlike Nb^{30+} 2p-4d lines at 4008.4 and 4011.3 mÅ, and some weaker lines from the magnesiumlike and fluorinelike charge states. A synthetic spectrum, generated

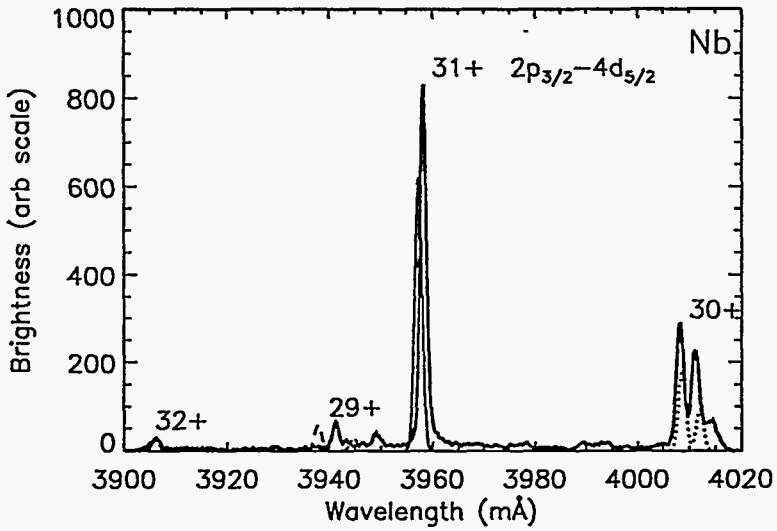

Figure 2: 2p-4d transitions in Nb^{29+} - Nb^{32+}. Theoretical lines for neonlike Nb^{31+} (solid), Nb^{30+} (dotted), Nb^{29+} (dashed) and Nb^{32+} (dash-dot-dash) are shown at the bottom, where the relative intensities within a given charge state are proportional to the oscillator strengths of each transition.

using calculated wavelengths[11], typical instrumental and Doppler line widths, and line amplitudes proportional to the oscillator strengths[11] within a given charge state, is shown at the bottom of the figure. The observed niobium lines are within 1 mÅ of the calculated wavelengths[11]. Wavelength calibration was obtained from several nearby Ar^{16+} lines[26,27], S^{14+} lines[26] and S^{15+} lines[28]. A calibration spectrum showing several sulphur lines is shown in Fig.3. This spectrum includes the (unresolved) Lyman β doublet and the $1s^2$-1snp series in S^{14+} with n between 5 and 13. Calculated wavelengths and radiative transition probabilities for this series are given in Table I.

Another strong neonlike Nb^{31+} line, the $2p^6$ - $(2p^5)_{\frac{1}{2}}4d_{\frac{3}{2}}$ transition at 3843.8 mÅ, is shown in Fig.4a. Also prominent in the figure are the 2p-4d lines at 3892.8 and 3822.9 mÅ, from sodium- and fluorinelike niobium, respectively. The corresponding 2p-5d transitions are shown in Fig.4b. At the bottom of each figure is a synthetic spectrum and the wavelength agreement is very good.

For higher n transitions in neonlike systems, the upper levels of certain lines in the $2p^6$ - $(2p^5)_{\frac{3}{2}}nd_{\frac{5}{2}}$ series and the $2p^6$ - $(2p^5)_{\frac{1}{2}}nd_{\frac{3}{2}}$ series can have nearly identical energies, giving rise to significant configuration interaction. In particular, the effect is seen in the enhancement of the intensity of the $2p^6$

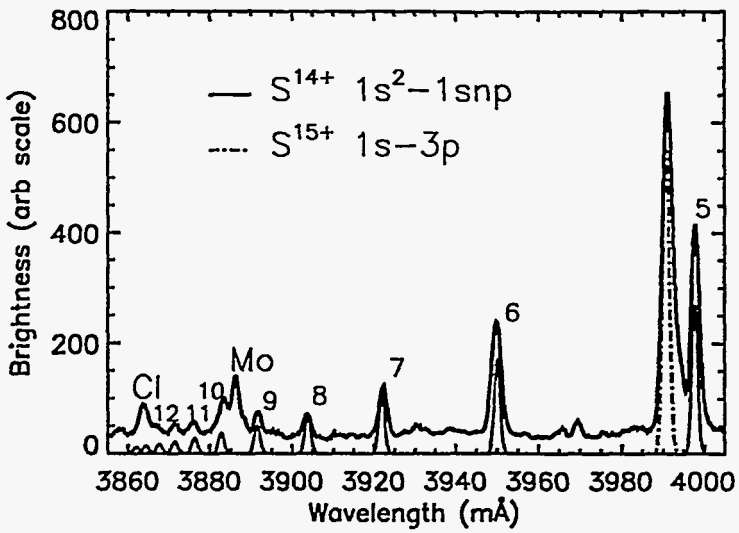

Figure 3: $1s^2$-1snp transitions in S^{14+} with n between 5 and 12. Also apparent is the Lyman β doublet of S^{15+}, a 2p-4s line of Mo^{32+} at 3886.3 mÅ, and a satellite of Cl^{15+} K_β at 3863.7 mÅ.

Table 1: Calculated $1s^2$-1snp transition wavelengths and radiative transition probabilities for heliumlike S^{14+}.

Transition	wavelength (mÅ)	A (10^{12}/s)
$1s^2\ ^1S_0$ - 1s4p $^1P_1$	4088.46	7.28
$1s^2\ ^1S_0$ - 1s5p $^1P_1$	3997.73	3.63
$1s^2\ ^1S_0$ - 1s6p $^1P_1$	3950.10	2.07
$1s^2\ ^1S_0$ - 1s7p $^1P_1$	3921.92	1.29
$1s^2\ ^1S_0$ - 1s8p $^1P_1$	3903.84	.860
$1s^2\ ^1S_0$ - 1s9p $^1P_1$	3891.54	.602
$1s^2\ ^1S_0$ - 1s10p $^1P_1$	3882.79	.438
$1s^2\ ^1S_0$ - 1s11p $^1P_1$	3876.34	.328
$1s^2\ ^1S_0$ - 1s12p $^1P_1$	3871.45	.252
$1s^2\ ^1S_0$ - 1s13p $^1P_1$	3867.66	.198

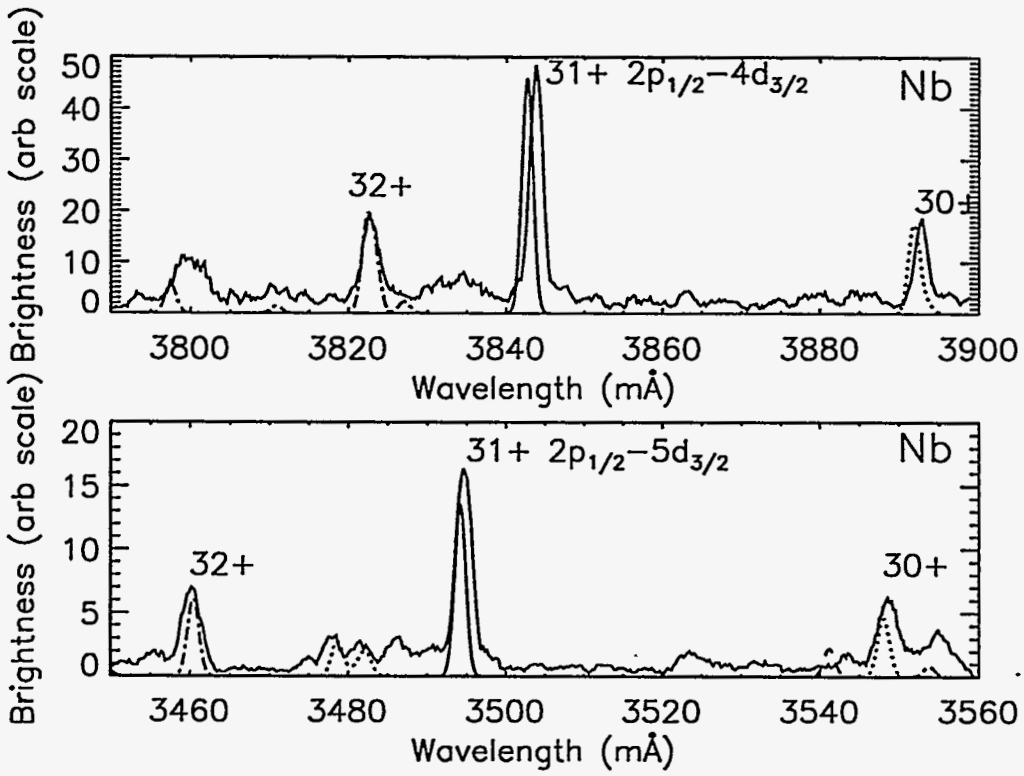

Figure 4: (a) 2p-4d and (b) 2p-5d transitions in neonlike Nb^{31+} (solid), Nb^{30+} (dotted) and Nb^{32+} (dash-dot dash).

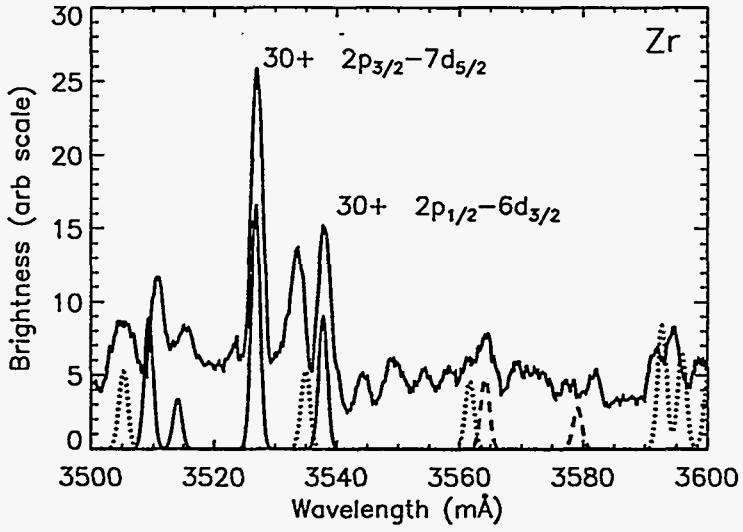

Figure 5: $2p_{\frac{3}{2}}$ - $7d_{\frac{5}{2}}$ and $2p_{\frac{1}{2}}$ - $6d_{\frac{3}{2}}$ transitions in neonlike Zr^{30+}, and the calculated neonlike (solid), sodiumlike (dotted) and fluorinelike (dashed) lines. Also shown are 2s-5p transitions in Zr^{30+} (solid) at 3510.3 and 3515.1 mÅ.

- $(2p^5)_{\frac{3}{2}}7d_{\frac{5}{2}}$ transition at the expense of the $2p^6$ - $(2p^5)_{\frac{1}{2}}6d_{\frac{3}{2}}$ transition[10,11] in Mo^{32+}, where the difference in the upper state energy levels is 3.5 eV, and the interaction is quite large. A spectrum of these two lines in Zr^{30+} is shown in Fig.5. In the case of zirconium, the separation is 11 eV (11 mÅ) and there is little configuration interaction at all (the two lines are within a factor of 2 in intensity). This effect is summarized in Fig.6a where the calculated oscillator strengths of the $2p^6$ - $(2p^5)_{\frac{3}{2}}6d_{\frac{5}{2}}$, the $2p^6$ - $(2p^5)_{\frac{1}{2}}6d_{\frac{3}{2}}$, the $2p^6$ - $(2p^5)_{\frac{3}{2}}7d_{\frac{5}{2}}$ and the $2p^6$ - $(2p^5)_{\frac{1}{2}}7d_{\frac{3}{2}}$ lines are plotted as a function of atomic number. The oscillator strengths of the $2p^6$ - $(2p^5)_{\frac{3}{2}}6d_{\frac{5}{2}}$ lines and the $2p^6$ - $(2p^5)_{\frac{1}{2}}7d_{\frac{3}{2}}$ lines are relatively insensitive to atomic number. The magnitude of the configuration interaction between the $2p^6$ - $(2p^5)_{\frac{1}{2}}6d_{\frac{3}{2}}$ level and the $2p^6$ - $(2p^5)_{\frac{3}{2}}7d_{\frac{5}{2}}$ level is quite apparent; as the atomic number increases from Y to Mo, the g*f value of the $7d_{\frac{5}{2}}$ line increases while the value of the $6d_{\frac{3}{2}}$ line decreases. At technetium (Z=43), this effect dramatically switches; for Tc and above, the $2p^6$ - $(2p^5)_{\frac{1}{2}}6d_{\frac{3}{2}}$ line is at shorter wavelength and the $2p^6$ - $(2p^5)_{\frac{3}{2}}7d_{\frac{5}{2}}$ line is the *weaker* of the two. The wavelength differences between the two levels is shown in Fig.6b.

For the electron temperatures of Alcator C-Mod, palladium can just reach the neonlike state, and the lower charge states are present in abundance.

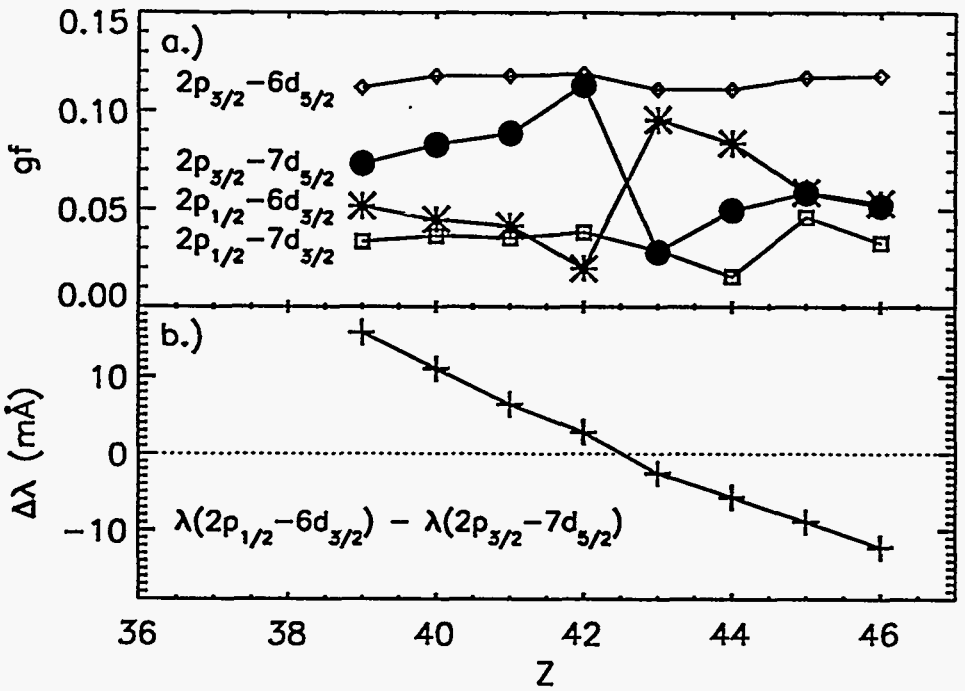

Figure 6: Calculated oscillator strengths (a) of 2p-6d and 2p-7d transitions and calculated wavelength differences (b) between $2p_{\frac{1}{2}}$ - $6d_{\frac{3}{2}}$ transitions and $2p_{\frac{3}{2}}$ - $7d_{\frac{5}{2}}$ transitions as a function of atomic number Z.

Table 2: Calculated neonlike 2p-nd E1 transition wavelengths and oscillator strengths for n = 6 and 7 in Y^{29+}, Tc^{33+}, Ru^{34+} and Rh^{35+}. The upper level designations in the first column are indicated by three jj-coupled orbitals where '-' indicates $l - s$ coupling and '+' indicates $l + s$ coupling: the first two orbitals show the occupancy of the $2p_{\frac{1}{2}}$ and $2p_{\frac{3}{2}}$ subshells, respectively, and the third orbital is where the 2p-electron has been promoted.

Upper level	Y^{29+}		Tc^{33+}		Ru^{34+}		Rh^{35+}	
	λ_T (mÅ)	g*f	λ_T (mÅ)	g*f	λ_T (mÅ)	g*f	λ_T (mÅ)	g*f
$(2p_-)^2(2p_+)^3 6d_+$ J=1	3856.8	.112	3055.4	.111	32894.1	.111	2744.3	.117
$(2p_-)(2p_+)^4 6d_-$ J=1	3765.6	.0516	2967.1	.0955	2806.7	.0836	2657.7	.0587
$(2p_-)^2(2p_+)^3 7d_+$ J=1	3749.9	.0733	2969.7	.0280	2812.4	.0494	2666.6	.0583
$(2p_-)(2p_+)^4 7d_-$ J=1	3663.0	.0334	2885.7	.0289	2729.4	.0155	2584.3	.0460

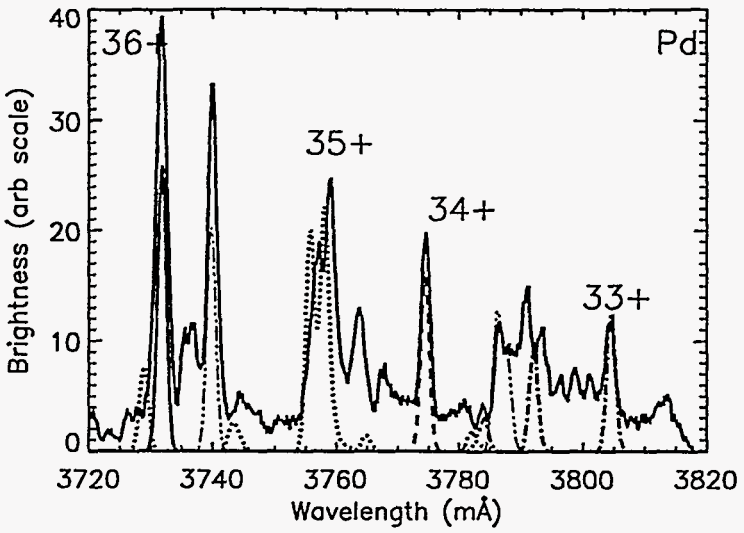

Figure 7: 2p-3d transitions in Pd^{33+} - Pd^{36+}. Theoretical lines for neonlike Pd^{36+} (solid), Pd^{35+} (dotted), Pd^{34+} (dashed) and Pd^{33+} (dash-dot-dash) are shown at the bottom, where the relative intensities within a given charge state are proportional to the oscillator strengths of each transition. Molybdenum transitions are shown by the thin dash-dot-dot-dot-dash lines.

Shown in Fig.7 is a spectrum of Pd 2-3 transitions in the vicinity of the $2p^6$ - $(2p^5)_{\frac{1}{2}}3d_{\frac{3}{2}}$ line at 3731.7 mÅ. The corresponding lines in Pd^{35+}, Pd^{34+} and aluminumlike Pd^{33+} are clearly identified.

Conclusions

X-ray transitions in the magnesiumlike through fluorinelike charge states in zirconium, niobium, molybdenum and palladium have been observed from Alcator C-Mod plasmas. Line identifications have been made by comparison to the results of *ab initio* calculations and overall wavelength agreement is very good. The magnitude of the configuration interaction between the $(2p^5)_{\frac{1}{2}}6d_{\frac{3}{2}}$ level and the $(2p^5)_{\frac{3}{2}}7d_{\frac{5}{2}}$ level has been calculated as a function of atomic number for $39 \leq Z \leq 46$. 2p-3d transitions in aluminumlike Pd^{33+} have also been identified.

Acknowledgements

The authors would like to thank F. Bombarda for assistance with the spectrometer system, J. Irby for electron density measurements, A. Hubbard for

electron temperature measurements and the Alcator C-Mod operations group for expert running of the tokamak. Work supported at MIT by DoE Contract No. DE-AC02-78ET51013 and at LLNL by DoE Contract No. W-7405-ENG-48.

References

[1] E.Källne, J.Källne and R.D.Cowan, Phys. Rev. A **27**, 2682 (1983).
[2] P.Beiersdorfer et al., Phys. Rev. A **34**, 1297 (1986).
[3] P.Beiersdorfer et al., Phys. Rev. A **37**, 4153 (1988).
[4] E.V.Aglitskii et al., Physica Scripta **40**, 601 (1989).
[5] P.Beiersdorfer et al., Phys. Rev. Lett. **65**, 1995 (1990).
[6] R.Hutton et al., Phys. Rev. A **44**, 1836 (1991).
[7] M.B.Schneider et al., Phys. Rev. A **45**, R1291 (1992).
[8] Steven Elliott et al., Phys. Rev. A **47**, 1403 (1993).
[9] P.Beiersdorfer et al., Physica Scripta **51**, 322 (1995).
[10] J.E.Rice et al., Phys Rev A **51**, 3551 (1995).
[11] J.E.Rice et al., accepted for publication in Phys. Rev. A (1995).
[12] D.L.Matthews et al., Phys. Rev. Lett., **54**, 110 (1985).
[13] M.D.Rosen et al., Phys. Rev. Lett., **54**, 106 (1985).
[14] A.L. Osterheld et al., J. Quant. Spectrosc. Radiat. Transfer, **51**, No. 1/2, 263 (1994).
[15] P.Beiersdorfer, M.H.Chen, R.E.Marrs and M.Levine, Phys. Rev. A **41**, 3453 (1990).
[16] G.A.Chandler, M.H.Chen, D.D.Dietrich, P.O.Egan, K.P.Ziock, P.H.Mokler, S.Reusch and D.H.H.Hoffmann, Phys. Rev. A, **39**, 565 (1989).
[17] D.D.Dietrich, G.A.Chandler, P.O.Egan, K.P.Ziock, P.H.Mokler, S.Reusch and D.H.H.Hoffmann, Nucl. Instrum. Methods B, **24/25**, 301 (1987).
[18] E. Avgoustoglou, W.R. Johnson, Z.W. Liu and J. Sapirstein, Phys. Rev. A, **51**, 1196 (1995).
[19] W.R. Johnson, J. Sapirstein and K.T. Cheng, Phys. Rev. A, **51**, 297 (1995).
[20] I.H.Hutchinson et al., Phys. Plasmas **1**, 1511 (1994).
[21] R.D.Cowan, The Theory of Atomic Structure and Spectra, University of California Press, pp.433-434 (1981).
[22] M.A.Graf et al., Rev. Sci. Instrum. **66**, 636 (1995).
[23] J.E.Rice and E.S.Marmar, Rev. Sci. Instrum. **61**, 2753 (1990) .
[24] M.Klapisch, Comput. Phys. Commun. **2**, 269 (1971).
[25] M.Klapisch, J.L.Schwob, B.S.Fraenkel and J.Oreg, J. Opt. Soc. Am. **67**, 148 (1977).
[26] L.A.Vainshtein and U.I.Safronova, Physica Scripta **31**, 519 (1985).
[27] J.E.Rice, E.S.Marmar, E.Källne and J.Källne, Phys. Rev. A **35**, 3033 (1987).
[28] G.W.Erickson, J. Phys. Chem. Ref. Data **6**, 831 (1977).